Journal of Nuclear Materials 408 (2011) 125–128

Contents lists available at ScienceDirect

Journal of Nuclear Materials

journal homepage: www.elsevier.com/locate/jnucmat

Letter to the Editor

# Stress corrosion cracking in the heat-affected zone of A508 steel welds under high-temperature water

Wei-Chih Chung [a], Jiunn-Yuan Huang [b], Leu-Wen Tsay [c], Chun Chen [a,*]

[a] *Department of Materials Science and Engineering, National Taiwan University, Taipei 106, Taiwan*
[b] *Institute of Nuclear Energy Research, Lungtan 325, Taiwan*
[c] *Institute of Materials Engineering, National Taiwan Ocean University, Keelung 202, Taiwan*

ARTICLE INFO

*Article history:*
Received 28 September 2010
Accepted 25 October 2010

ABSTRACT

The influence of heat input on stress corrosion cracking (SCC) in the heat-affected zone (HAZ) of A508 steel welds was investigated. Constant extension rate tensile tests were conducted on notched round-bar specimens in simulated reactor coolant conditions to assess SCC performance. In multi-pass welds, the use of a low heat input resulted in a better SCC resistance than that of a high heat input due to the existence of a more refined microstructure.



## 1. Introduction

Dissimilar metal welding is widely used for joining low-alloy to stainless steel components in the nuclear power industry [1,2]. For such applications, Alloy 52, a nickel-based alloy, has been used as a buttering or filler metal in the dissimilar metal welds [3,4]. In multi-pass welding, the heat-affected zone (HAZ) of a weld undergoes microstructural changes due to the multiple thermal cycles. It is known that the heat input affects the thermal cycle and the transformation products in the HAZ of the weld. Consequently, the resistance to stress corrosion cracking (SCC) can be altered in the HAZ as a result of the weld heat input.

Environment-assisted cracking is one of the most common failure mechanisms of reactor pressure vessels after long-term services [5]. In the case of nozzle-to-pipe welds, large axial cracks initiated in the nickel-based weld metal and then propagated into the HAZ of the low-alloy steel nozzle have been observed [6]. Choi et al. also reported that A508 steel is susceptible to transgranular SCC in oxygenated water at temperatures ranging from 100 to 288 °C [7]. Although many investigations have conducted research on SCC of dissimilar metal welds [8,9], little attention has been paid to evaluate the SCC behavior in the HAZ.

The aim of this study was to investigate the influence of heat input on SCC resistance in the HAZ of A508 welds using Alloy 52 filler metal. The susceptibility to SCC in the HAZ region of the welds was evaluated on notched round-bar specimens by performing constant extension rate tensile (CERT) tests in a simulated water reactor environment. In addition, the dependence of the HAZ grain size and microstructure on the weld heat input is discussed.

## 2. Materials and experimental procedures

The materials used in this experiment were A508 Class 2 forged steel (0.17 wt% C, 0.67 wt% Ni, 0.37 wt% Cr, 0.92 wt% Mn, 0.66 wt% Mo, 0.03 wt% V and balanced Fe) and Alloy 52 (0.04 wt% C, 29.05 wt% Cr, 9.47 wt% Fe, 0.27 wt% Mn, 0.05 wt% Mo, and balanced Ni) filler wire that was 2.4 mm in diameter. The steel was cut and solution-treated at 900 °C for 6 h, then quenched in water and finally tempered at 680 °C for 4 h. Fig. 1 shows the schematic diagram of the joint design and the welding sequence. The A508 specimens ($150 \times 50 \times 15$ mm) were buttered with Alloy 52 prior to filling a single 55° bevel joint using the multi-pass gas tungsten arc welding method. The welding parameters included a voltage of 12 V, a speed of about 132 mm/min, a preheat temperature of 150 °C and a current of either 140 or 175 A. For a given weld, all weld passes (Fig. 1) were processed with similar welding parameters regardless of whether the higher current could be used to fill the butt joints. After welding, the welds were subjected to post-weld heat treatment (PWHT) at 621 °C for 24 h and were inspected by X-ray before the SCC tests.

Fig. 2 shows the configuration of the notched round-bar specimen used in the experiment, where a circumferential V-notch (notch radius of 0.025 mm) was introduced 1 mm away from the vertical weld interface within the HAZ (Fig. 1). The CERT tests were conducted in pure water (about 7 wppm dissolved oxygen) at 300 °C and 10 MPa to simulate coolant conditions in a nuclear reactor. The CERT tests were conducted with two extension rates, i.e. $3 \times 10^{-4}$ mm/s (fast) and $1 \times 10^{-6}$ mm/s (slow), to study the influence of the environment on the SCC performance of two different heat input (764 and 955 J/mm) specimens, namely the low and high heat input specimens. For the HAZ specimen welded with a specified heat input, a fast CERT test represented little or no environmental contribution to the SCC, whereas a slow CERT test

* Corresponding author. Tel.: +886 2 33661308; fax: +886 2 23634562.
*E-mail address:* gchen@ntu.edu.tw (C. Chen).

0022-3115/$ - see front matter 
doi:10.1016/j.jnucmat.2010.10.052

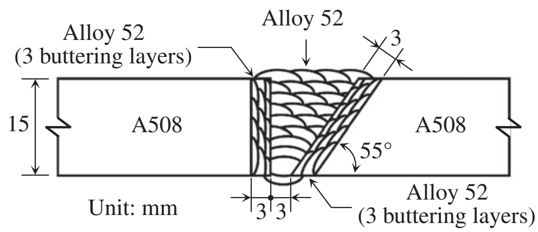


**Fig. 1.** Schematic diagram showing the A508 multi-pass welds using an Alloy 52 filler metal.

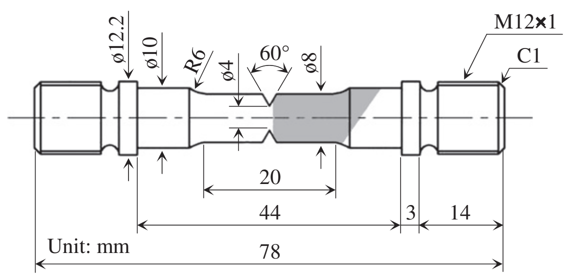


**Fig. 2.** Dimensions of the notched tensile specimen for the SCC test. Note that the shaded area is the weld metal.

represented a corrosion effect. As a result, the cracking susceptibility in terms of the percentage loss in the notched tensile strength (NTS) of a given specimen can be expressed as follows:

$$\text{NTS loss }(\%) = \frac{\text{NTS (fast)} - \text{NTS (slow)}}{\text{NTS (fast)}} \times 100\%$$

For microstructural observations, the HAZ specimens were etched using a 4% nital solution and examined with a scanning electron microscope (SEM). In addition, the fracture surfaces of the specimens after the CERT tests under the slow and fast extension rates were compared with a focus on regions that exhibited SCC fractures.

## 3. Results and discussion

The microstructures of the A508 base metal after PWHT consisted primarily of tempered martensite and bainite (Fig. 3a). For simplicity, if not specified, the HAZ specimens were in the PWHT condition in the following discussion. In comparison with the base metal, the microstructures in the HAZ of the A508 multi-pass welds were refined and had a mixture of bainite and ferrite regardless of the heat input. However, the low heat input specimen exhibited finer microstructures (Fig. 3b) than the high heat input specimen (Fig. 3c) due to a faster cooling rate and lower peak temperature during the weld thermal cycles. Fig. 3 also reveals significant differences in grain size between the base metal and the HAZ specimens. At high magnification, the precipitation of carbides at the ferrite grain boundaries was observed for the HAZ specimens after the PWHT but not found in the as-welded condition. The microhardness profiles of the weld cross-sections (Fig. 4) also revealed a lower hardness in the HAZ of the high heat input specimen, which was consistent with the microstructural observations, i.e. a lower hardness was associated with a coarser grain structure. It was noted that a circumferential notch in the CERT specimen was located around the highest hardness region in the HAZ for different heat input specimens. In addition, carbon migration from the A508 base metal to the Alloy 52 weld metal near the weld interface was observed after the PWHT.

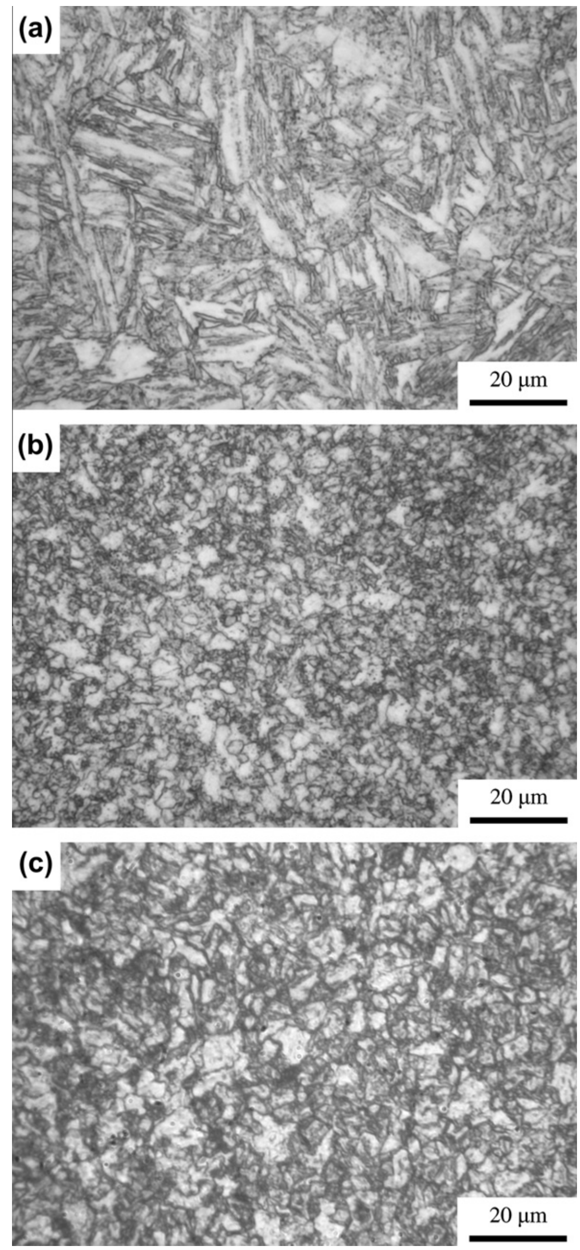


**Fig. 3.** SEM micrographs of the specimens after the PWHT: (a) A508 base metal; (b) the HAZ specimen with a low heat input; and (c) the HAZ specimen with a high heat input. Note that the microstructures shown in (b) and (c) are located 1 mm away from the weld interface.

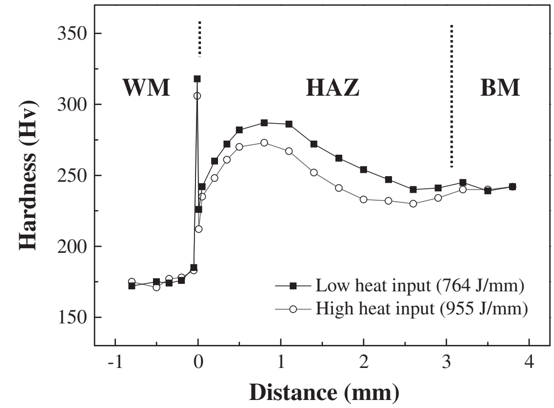


**Fig. 4.** Microhardness distribution of A508 steel welds after the PWHT.

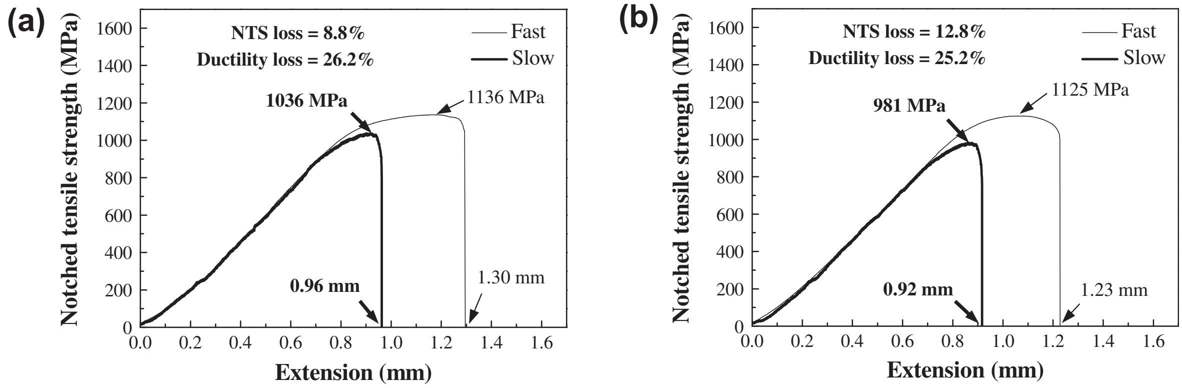


**Fig. 5.** Stress-extension curves of the CERT tests for the HAZ specimens with a heat input of (a) 764; and (b) 955 J/mm.

Fig. 5 shows the CERT results of the HAZ specimens for the two heat inputs. The stress-extension curves indicate that the high heat input specimen exhibited lesser NTS than the low heat input specimen, particularly at the slow extension rate. The NTS and ductility losses in the low heat input specimen were 8.8% and 26.2%, respectively. For the high heat input specimen, the NTS loss (12.8%) was higher, but the ductility loss (25.2%) seemed comparable with the low heat input specimen. The NTS loss has been used to study the susceptibility to environment-assisted cracking of a number of high-strength steels [10,11]. The results described above clearly indicate that the NTS loss is also suitable to assess the relative susceptibility to SCC in the HAZ.

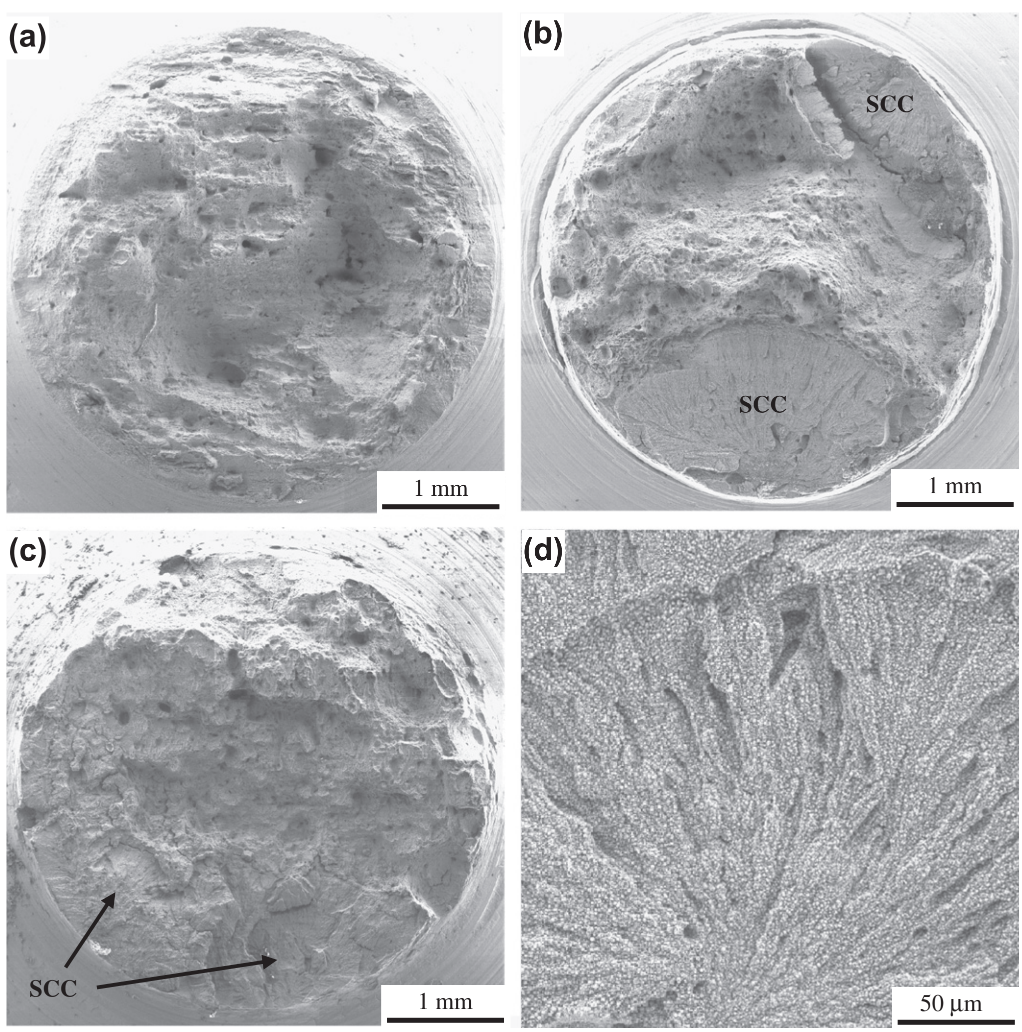


**Fig. 6.** Fractographs of the HAZ specimens after the CERT tests: (a) macroview of the high heat input specimen tested at $3 \times 10^{-4}$ mm/min; (b) macroview of the high heat input specimen tested at $1 \times 10^{-6}$ mm/min; (c) macroview of the low heat input specimen tested at $1 \times 10^{-6}$ mm/min; and (d) typical feather-like patterns in the transgranular SCC area.

A circumferential notch in a round-bar tensile specimen radically changes the stress distribution, causing a crack to grow inward. During the slow extension rate tests in high-temperature water, the area near the root of the notched tensile specimen was affected the most by the SCC, and a change in fracture modes was expected. Fig. 6a and b show typical fractographs of the high heat input specimens after the CERT tests at the fast and slow extension rates, respectively. The high heat input specimen that was tested at the slow rate exhibited obvious fan-shaped areas of the transgranular SCC fracture (marked SCC in Fig. 6b) on the fracture surface [12], while a similar specimen tested at the fast rate did not reveal any transgranular SCC (Fig. 6a). In the low heat input specimen that was tested at the slow rate, a reduced area of transgranular SCC was observed (Fig. 6c), where the fan-shaped fracture morphology was obscured at low magnification. Other than that, the fracture surfaces of the HAZ specimens consisted of mainly dimple fractures outside the SCC regions. The transgranular SCC areas of both specimens had similar fracture appearance and exhibited typical feather-like patterns (Fig. 6d). However, the area of feather-like patterns on the fracture surface in the low heat input specimen was less than that in the high heat input specimen. It should be mentioned that after the CERT tests, the fracture surfaces were covered with corrosion products (mostly magnetite), which might have caused the difficulties in SEM observation. It was concluded from the CERT results of the HAZ specimens in high-temperature water that the use of low heat input for welding of an A508 steel was beneficial to SCC resistance. The improvement could be attributed to the refined microstructures as discussed previously.

## 4. Summary

The notched round-bar specimen with a circumferential notch at the HAZ of an A508 steel weld was found to be useful in determining the SCC behavior of a narrow region of the weld. Slow extension rate tests under simulated reactor coolant conditions could be used to rank SCC resistance of the HAZ specimens, which were processed at two different heat inputs. The SCC resistance, in terms of NTS loss, clearly indicated that the low heat input was beneficial to the SCC resistance in the HAZ of A508 steel welds. Apparently, a more refined structure in the HAZ of the multi-pass welds was attributed to the low heat input. The HAZ microstructures of A508 welds with different heat inputs were similar and consisted of mainly bainite and ferrite; however, the low heat input specimen had a finer grain size than the high heat input specimen.

## Acknowledgments

The authors gratefully acknowledge financial support of this investigation by the ROC National Science Council (Contract Numbers NSC99-NU-E-002-001 and NSC98-NU-E-002-001) and technical assistance from the Institute of Nuclear Energy Research.

## References

[1] N. Taylor, C. Faidy, P. Gilles, Assessment of Dissimilar Weld Integrity: Final Report of the NESC-III, EUR 22510 EN, 2006.
[2] J.W. Kim, K. Lee, J.S. Kim, T.S. Byun, J. Nucl. Mater. 384 (2009) 212–221.
[3] J.N. DuPont, J.C. Lippold, S.D. Kiser, Welding Metallurgy and Weldability of Nickel-Base Alloy, Wiley & Sons Inc., New Jersey, 2009.
[4] S.D. Kiser, E.B. Hinshaw, in: Focus on Nuclear Power Generation 2005, 2005, pp. 21–26.
[5] H.P. Seifert, S. Ritter, J. Nucl. Mater. 372 (2008) 114–131.
[6] A.R. McIlree, EPRI Interim Report, TP-1001491-NP, Part. 1 (Non-proprietary Information), April 2001.
[7] H. Choi, F.H. Beck, Z. Szklarska-Smialowska, D.D. Macdonald, Corrosion 38 (1982) 136–144.
[8] D.I. Roberts, R.H. Ryder, R. Viswanathan, J. Press Vess. Technol. 107 (1985) 247–254.
[9] F. Vaillant, J. Boursier, L. Legras, B. Yrieix, E. Lemaire, J. Champredonde, C. Amzallag, in: Proc. 13th Int. Conf. on Environmental Degradation of Materials in Nuclear Power System – Water Reactors (Whistler, British Columbia, August 19–23, 2007).
[10] L.W. Tsay, H.L. Lu, C. Chen, Corros. Sci. 50 (2008) 2506–2511.
[11] L.W. Tsay, Y.S. Ding, M.F. Chiang, C. Chen, J. Nucl. Mater. 385 (2009) 538–544.
[12] G.F. Li, E.A. Charles, J. Congleton, Corros. Sci. 43 (2001) 1963–1983.